

Multicolour Optical Surface Brightness Profiles Decomposition of the Seyfert Galaxies III Zw 2, Mrk 506 and Mrk 509*

L. Slavcheva-Mihova, B. Mihov, G. Petrov and V. Kopchev

*Institute of Astronomy, Bulgarian Academy of Sciences,
72 Tsarigradsko Chausse Blvd., 1784 Sofia, Bulgaria
lslav, bmihov, petrov@astro.bas.bg*

May 2006

Abstract

We present the results of the $UBVR_{\text{C}}I_{\text{C}}$ surface brightness profiles decomposition of the Seyfert galaxies III Zw 2, Mrk 506 and Mrk 509. The profiles were modelled as a sum of a Gaussian, a Sérsic law and an exponent. A Ferrers bar and a Gaussian ring were added to the model profiles of III Zw 2 and Mrk 506, respectively. The parameters and the total magnitudes of the structural components were derived.

1 Introduction

We present here the first results of an outgoing study aimed to do a detailed decomposition of Seyfert galaxies $UBVR_{\text{C}}I_{\text{C}}$ surface brightness profiles (hereafter SBPs). Our advantages over Seyfert galaxies SBP decomposition found in the literature are the following: (1) we model explicitly the active nucleus in opposition to some authors who avoid nucleus modelling (e.g. [1]), (2) we use Sérsic

*Based on observations obtained at the Rozhen National Astronomical Observatory of Bulgaria operated by the Institute of Astronomy, Bulgarian Academy of Sciences.

rather than de Vaucouleurs law for bulge, (3) we use a truncated exponential law defined in [2] along with a pure exponent in disk modelling, and (4) we model bar/oval/lens/ring components that have been generally skipped by Seyfert galaxies SBPs decomposers (e.g. [3]).

All galaxies to be decomposed were observed at Rozhen NAO of Bulgaria with the 2-m telescope and Photometrics AT200 CCD camera ($0.309 \text{ arcsec px}^{-1}$) through a standard Johnson-Cousins $UBVR_{\text{C}}I_{\text{C}}$ set of filters. The SBPs of the galaxies were extracted fitting ellipses to the galaxian isophotes by means of `FIT/ELL3` command of the `SURFPHOT` context of ESO-MIDAS package (see [4] for details).

Our first decomposition results concern the Seyfert galaxies III Zw 2 (Sy1.0), Mrk 506 (Sy1.5) and Mrk 509 (Sy1.2); the Seyfert types are taken from NED.

2 Models and Methods

Our basic model SBP is a sum of (1) a Gaussian with a fixed FWHM to represent the nucleus (the only free parameter is the central surface brightness), (2) a Sérsic law [5] with free parameters μ_{eff} – the effective surface brightness, r_{eff} – the effective radius, and n – the power-law index, to represent the bulge and (3) an exponent [6] with free parameters μ_{cen} – the central surface brightness, and r_{scl} – the scale length, to represent the disk. Bulge and disk model SBPs were convolved with a Gaussian PSF to simulate the seeing effects on the profiles according to [7, 8]. Note that if the frame PSF is not circular then the FWHM of the convolution Gaussian is set to the PSF's mean FWHM along the minor axis and the FWHM of the nuclear Gaussian is set to the PSF's mean FWHM along the major axis (the mean FWHM of the stellar images for each frame was determined fitting a 2D Gaussian to a number of field stars employing `CENTER/IQE` command within ESO-MIDAS).

We added (1) a Ferrers model profile [9] with free parameters μ_{cen} – the central surface brightness, r_{end} – the profile length, and m – the power-law index, to account for the bar¹ in III Zw 2, and (2) a displaced Gaussian model profile [10] with free parameters μ_{cen} – the central surface brightness, r_{cen} – the position (or displacement) of the Gaussian centre, and \mathcal{FW} – the FWHM, to account for the ring in Mrk 506 (the galaxy has $SAB(r)a$ morphology according to NED).

The figure-of-merit function that is minimized is equal to the unweighted sum of the squared differences between the observed and the model SBPs per degree

¹The bar manifests in about 0.25 rise of the ellipticity and an almost constant position angle.

of freedom, ν :

$$\Delta_\nu^2(\mathbf{p}) = \nu^{-1} \sum_{i=1}^N \left[\mu_i^{\text{OBS}} - \mu_i^{\text{MOD}}(\mathbf{p}) \right]^2, \quad (1)$$

where \mathbf{p} is the P -element vector of the free model parameters to be fitted. The initial value of the degrees of freedom is defined as $\nu_0 = N - P$, where N and P are the number of the profile data points and the number of the free parameters, \mathbf{p} , to be fitted, respectively. Note that corrections to ν_0 could be done for the presence of (1) zero-weighted profile data points, N_{zero} , and/or (2) fixed parameters, P_{fix} , so the actual value of ν becomes $\nu = \nu_0 - N_{\text{zero}} + P_{\text{fix}}$, and the corrected value of ν enters Eq. 1. The minimization of $\Delta_\nu^2(\mathbf{p})$ was performed employing Levenberg-Marquardt algorithm [11]. The initial guess parameters were estimated by eye overplotting the observed and the model profiles and changing the parameters manually to get a good correspondence between them. After that, a P -dimensional *valley* $[\mathbf{p} - \delta\mathbf{p}^-, \mathbf{p} + \delta\mathbf{p}^+]$ around the initial guess parameters was constructed; here $\delta\mathbf{p}^{+/-}$ are the allowed parameters' deviations from their initial guess values in both directions (these deviations could be different for each parameter). Next, a number of decomposition cycles were run: in each cycle the actual initial guess parameters were picked up randomly from the uniformly distributed parameters in the *valley* defined above. This procedure helped us in isolating the global minimum among $\Delta_\nu^2(\mathbf{p})$ values – the larger the number of the random cycles is, the bigger the probability to find the global minimum becomes. The number of random cycles could vary depending on the complexity of the profile to be decomposed – more complicated profiles could require up to several hundreds of random cycles. After the minimization cycles were completed a histogram of $\Delta_\nu^2(\mathbf{p})$ values was built and the minimum corresponding to the most frequently occurring $\Delta_\nu^2(\mathbf{p})$ was selected. If the parameters corresponding to this minimum behaved themselves well and if this minimum had the lowest value of $\Delta_\nu^2(\mathbf{p})$ then it was assumed to be the global one with $\Delta_\nu^2(\mathbf{p}_{\text{min}}) = \Delta_{\nu, \text{min}}^2$; the correspondence between the parameter values obtained after decomposition of different observing runs profiles could be used as a further check of the minimum found (see Table 1). If some of the parameters corresponding to the most frequently occurring minimum had unacceptable values (e.g. very small or very large), then this minimum was rejected and a new global minimum was searched for among the remaining random cycles results. If there were minima with $\Delta_\nu^2(\mathbf{p})$ values lower than $\Delta_\nu^2(\mathbf{p})$ of the most frequently occurring minimum then these minima were checked one by one; in all cases we found that the parameters corresponding to these minima had unacceptable values, i.e. these minima were local ones.

3 Results

At the end of the selected objects decomposition the best-fit parameters were obtained (listed in Table 1) and, based on them, the total magnitudes of the structural components were computed (listed in Table 2). We list only the total magnitudes for the nuclear Gaussian because its central surface brightness is strongly dependent on the seeing and does not allow straightforward comparison of the results obtained at nights with different seeing conditions. The structural parameter(s) and/or the total magnitude(s) that could not be derived from the decomposition are marked in the tables. The errors of the parameters are 1σ uncertainties as resulting from the fitting algorithm and they should be considered as approximate ones. More reliable estimate of the parameter errors could be obtained through Monte Carlo simulations or a bootstrap analysis. The mean FWHM along the minor axis of the stellar images, $\overline{FW}_{\text{PSF}}$, that was used in the model SBPs convolution and the values of $\sigma_{\text{fit}} = (\Delta_{\nu, \text{min}}^2)^{0.5}$ are listed in Table 2 as well. The civil date and the name of the decomposed object are listed in the tables using the following code: 1a – September 9/10, 1997 III Zw 2; 1b – June 1/2, 1997 Mrk 506; 2b – July 18/19, 1998 Mrk 506; 1c – July 10/11, 1997 Mrk 509; 2c – September 8/9, 1997 Mrk 509; 3c – July 20/21, 1998 Mrk 509. Corresponding Johnson-Cousins filter is shown along with the date and the object code. We list the parameters of the bar in III Zw 2 and of the ring in Mrk 506 in Table 3 and Table 4, respectively. Note that the magnitudes and the surface brightnesses listed in the tables have not been corrected for the Galactic absorption and cosmological dimming; k - and evolution corrections have not been applied as well.

The observed SBPs and the decomposed profiles of the structural components of III Zw 2, Mrk 506 and Mrk 509 are shown in Fig. 1, Fig. 2 and Fig. 3, respectively, along with the residual profiles equal to $\mu^{\text{OBS}} - \mu^{\text{MOD}}(\mathbf{p}_{\text{min}})$. We show the decompositions with the smallest σ_{fit} among the different filters and observing runs for each galaxy (see Table 2).

We list in Table 3 the length of the bar in III Zw 2 obtained from the $BVR_{\text{C}}I_{\text{C}}$ ellipticity profiles using (1) a maximum ellipticity criterion – the bar length, $l_{\text{bar}}^{(\text{max})}$, corresponds to the point of maximal ellipticity, and (2) a minimum ellipticity criterion – the bar length, $l_{\text{bar}}^{(\text{min})}$, corresponds to the point of minimal ellipticity next to the ellipticity maximum, so one has $l_{\text{bar}}^{(\text{min})} > l_{\text{bar}}^{(\text{max})}$ by definition. One could see that $l_{\text{bar}}^{(\text{min})}$ agree well with the bar length, r_{end} , obtained from the SBPs decomposition, while $l_{\text{bar}}^{(\text{max})}$ underestimates r_{end} (cf. [12]).

BVI_{C} profiles decomposition of Mrk 509 was recently presented by [3] where

Table 1: Bulge (^B) and disk (^D) structural parameters for III Zw 2, Mrk 506 and Mrk 509. The errors of the parameters are shown as a superscript index to the corresponding values.

| Code | $\mu_{\text{eff}}^{\text{B}}$ [mag / \square''] | $r_{\text{eff}}^{\text{B}}$ [''] | n^{B} | $\mu_{\text{cen}}^{\text{D}}$ [mag / \square''] | $r_{\text{scl}}^{\text{D}}$ [''] |
|------------------|--|---------------------------------------|------------------------|--|---------------------------------------|
| 1aB | 18.762 ^{0.193} | 0.849 ^{0.058} | 0.976 ^{0.099} | 23.380 ^{0.028} | 5.138 ^{0.044} |
| 1aV | 18.182 ^{0.143} | 0.847 ^{0.047} | 1.117 ^{0.104} | 22.001 ^{0.017} | 5.732 ^{0.033} |
| 1aR _C | 17.346 ^{0.315} | 0.784 ^{0.092} | 0.915 ^{0.186} | 21.146 ^{0.051} | 5.318 ^{0.085} |
| 1aI _C | 17.939 ^{0.340} | 1.114 ^{0.138} | 0.615 ^{0.177} | 20.312 ^{0.023} | 5.766 ^{0.042} |
| 2bU | 18.181 ^{0.210} | 1.003 ^{0.075} | 1.079 ^{0.140} | 21.404 ^{0.053} | 6.473 ^{0.124} |
| 1bB | — | — | — | 21.011 ^{0.010} | 6.222 ^{0.021} |
| 2bB | 19.825 ^{0.242} | 1.342 ^{0.153} | 0.316 ^{0.171} | 21.110 ^{0.023} | 6.185 ^{0.045} |
| 1bV | — | — | — | 20.227 ^{0.007} | 6.346 ^{0.013} |
| 2bV | 19.168 ^{0.107} | 1.292 ^{0.054} | 0.592 ^{0.077} | 20.172 ^{0.016} | 6.198 ^{0.031} |
| 1bR _C | 19.563 ^{2.958} | 1.287 ^{1.324} | 1.192 ^{1.694} | 19.579 ^{0.013} | 6.051 ^{0.022} |
| 2bR _C | 19.040 ^{0.043} | 1.473 ^{0.029} | 0.460 ^{0.036} | 19.628 ^{0.010} | 6.285 ^{0.018} |
| 1bI _C | 19.619 ^{0.050} | 2.057 ^{0.054} | 0.647 ^{0.083} | 19.161 ^{0.009} | 7.086 ^{0.023} |
| 2bI _C | 18.149 ^{0.034} | 1.298 ^{0.019} | 0.658 ^{0.036} | 18.939 ^{0.014} | 6.271 ^{0.030} |
| 3cU | 16.915 ^{0.201} | 1.545 ^{0.062} | 1.203 ^{0.042} | 21.343 ^{0.058} | 5.995 ^{0.119} |
| 1cB | 18.156 ^{0.086} | 1.429 ^{0.045} | 1.359 ^{0.065} | 21.933 ^{0.045} | 5.763 ^{0.092} |
| 2cB | 17.184 ^{0.091} | 0.981 ^{0.032} | 1.800 ^{0.063} | 21.848 ^{0.015} | 6.425 ^{0.033} |
| 3cB | 17.417 ^{0.212} | 1.450 ^{0.074} | 1.108 ^{0.044} | 21.411 ^{0.022} | 5.546 ^{0.042} |
| 1cV | 18.443 ^{0.066} | 1.880 ^{0.047} | 0.850 ^{0.044} | 20.514 ^{0.018} | 5.046 ^{0.025} |
| 2cV | 18.210 ^{0.082} | 1.585 ^{0.049} | 1.330 ^{0.075} | 20.910 ^{0.027} | 6.654 ^{0.070} |
| 3cV | 17.414 ^{0.144} | 1.400 ^{0.070} | 1.508 ^{0.096} | 20.877 ^{0.028} | 6.253 ^{0.060} |
| 1cR _C | 17.765 ^{0.034} | 1.717 ^{0.023} | 1.053 ^{0.028} | 20.051 ^{0.011} | 5.306 ^{0.017} |
| 2cR _C | 17.744 ^{0.049} | 1.633 ^{0.032} | 1.405 ^{0.049} | 20.550 ^{0.016} | 6.841 ^{0.035} |
| 3cR _C | 17.886 ^{0.072} | 1.877 ^{0.048} | 1.021 ^{0.048} | 20.107 ^{0.018} | 5.973 ^{0.039} |
| 1cI _C | 17.632 ^{0.030} | 1.957 ^{0.024} | 0.841 ^{0.028} | 19.217 ^{0.013} | 5.245 ^{0.022} |
| 2cI _C | 17.977 ^{0.045} | 1.960 ^{0.034} | 1.083 ^{0.042} | 19.614 ^{0.011} | 6.443 ^{0.024} |
| 3cI _C | 17.751 ^{0.057} | 2.036 ^{0.044} | 0.951 ^{0.049} | 19.356 ^{0.018} | 6.743 ^{0.049} |

Table 2: Nucleus (^N), bulge (^B) and disk (^D) total magnitudes for III Zw 2, Mrk 506 and Mrk 509. The errors of the magnitudes are shown as a superscript index to the corresponding values. The values of $\overline{\mathcal{FW}}_{\text{PSF}}$ and σ_{fit} are listed as well.

| Code | $\mu_{\text{tot}}^{\text{N}}$ [mag] | $\mu_{\text{tot}}^{\text{B}}$ [mag] | $\mu_{\text{tot}}^{\text{D}}$ [mag] | $\overline{\mathcal{FW}}_{\text{PSF}}$ ["] | σ_{fit} [mag / \square''] |
|-------------------|--|--|--|---|--|
| 1aB | $16.935^{0.113}$ | $16.435^{0.193}$ | $17.831^{0.028}$ | 1.575 | 0.025 |
| 1aV | $16.073^{0.060}$ | $15.797^{0.143}$ | $16.214^{0.017}$ | 1.560 | 0.017 |
| 1a R_{C} | $15.779^{0.186}$ | $15.222^{0.316}$ | $15.522^{0.051}$ | 1.311 | 0.045 |
| 1a I_{C} | $14.893^{0.121}$ | $15.227^{0.341}$ | $14.512^{0.023}$ | 1.428 | 0.047 |
| 2bU | $15.858^{0.120}$ | $15.446^{0.210}$ | $15.353^{0.053}$ | 1.816 | 0.013 |
| 1bB | $16.591^{0.010}$ | — | $15.046^{0.010}$ | 2.502 | 0.028 |
| 2bB | $16.725^{0.111}$ | $16.956^{0.244}$ | $15.158^{0.023}$ | 1.752 | 0.035 |
| 1bV | $16.314^{0.019}$ | — | $14.219^{0.007}$ | 2.350 | 0.009 |
| 2bV | $16.604^{0.082}$ | $16.150^{0.107}$ | $14.215^{0.016}$ | 1.516 | 0.015 |
| 1b R_{C} | $16.230^{1.186}$ | $16.239^{2.963}$ | $13.674^{0.013}$ | 2.360 | 0.014 |
| 2b R_{C} | $15.838^{0.023}$ | $15.838^{0.043}$ | $13.641^{0.010}$ | 1.753 | 0.007 |
| 1b I_{C} | $15.690^{0.037}$ | $15.554^{0.050}$ | $12.914^{0.009}$ | 2.293 | 0.007 |
| 2b I_{C} | $15.884^{0.037}$ | $15.077^{0.034}$ | $12.957^{0.014}$ | 1.459 | 0.006 |
| 3cU | $12.664^{0.074}$ | $13.190^{0.201}$ | $15.459^{0.058}$ | 2.711 | 0.037 |
| 1cB | $15.288^{0.063}$ | $14.541^{0.086}$ | $16.134^{0.045}$ | 2.141 | 0.020 |
| 2cB | $15.191^{0.063}$ | $14.247^{0.091}$ | $15.813^{0.015}$ | 1.861 | 0.016 |
| 3cB | $14.140^{0.145}$ | $13.869^{0.212}$ | $15.696^{0.022}$ | 2.420 | 0.024 |
| 1cV | $14.595^{0.035}$ | $14.454^{0.066}$ | $15.004^{0.018}$ | 1.877 | 0.031 |
| 2cV | $14.398^{0.034}$ | $14.381^{0.082}$ | $14.799^{0.027}$ | 1.653 | 0.022 |
| 3cV | $14.169^{0.076}$ | $13.793^{0.144}$ | $14.901^{0.028}$ | 2.204 | 0.014 |
| 1c R_{C} | $14.202^{0.020}$ | $13.874^{0.034}$ | $14.432^{0.011}$ | 1.777 | 0.017 |
| 2c R_{C} | $13.920^{0.022}$ | $13.823^{0.049}$ | $14.379^{0.016}$ | 1.491 | 0.023 |
| 3c R_{C} | $13.424^{0.023}$ | $13.816^{0.072}$ | $14.231^{0.018}$ | 2.252 | 0.015 |
| 1c I_{C} | $13.929^{0.020}$ | $13.560^{0.030}$ | $13.623^{0.013}$ | 1.797 | 0.019 |
| 2c I_{C} | $13.697^{0.019}$ | $13.785^{0.045}$ | $13.573^{0.011}$ | 1.977 | 0.014 |
| 3c I_{C} | $13.289^{0.022}$ | $13.537^{0.057}$ | $13.216^{0.018}$ | 1.954 | 0.017 |

Table 3: Bar parameters for III Zw 2. The bar lengths obtained from the ellipticity profiles employing the maximal and the minimal ellipticity criteria are listed in the last two columns for comparison with the bar length obtained from the SBPs decomposition.

| Code | μ_{cen} [mag / \square''] | r_{end} [''] | m | $l_{\text{bar}}^{(\text{max})}$ [''] | $l_{\text{bar}}^{(\text{min})}$ [''] |
|-------------------|---|----------------------------|-----------------|---|---|
| 1aB | $23.941^{0.043}$ | $11.430^{0.142}$ | $1.874^{0.116}$ | 7.978 | 11.350 |
| 1aV | $22.510^{0.034}$ | $11.258^{0.110}$ | $1.852^{0.091}$ | 6.991 | 11.214 |
| 1a R_{C} | $22.189^{0.111}$ | $11.906^{0.701}$ | $2.506^{0.536}$ | 6.726 | 12.145 |
| 1a I_{C} | $22.409^{0.140}$ | $9.468^{0.213}$ | $0.876^{0.190}$ | 6.824 | 11.252 |

a sum of a Gaussian, a de Vaucouleurs and a truncated exponent was used as a model SBP. We have not found evidence of Freeman type II profile in Mrk 509 to justify the usage of a truncated exponent. We have found a nearly exponential bulge, $n \approx 1$, in all three galaxies decomposed (see also [13, 14]).

Acknowledgments

This research has made use of the NASA/IPAC Extragalactic Database (NED) which is operated by the Jet Propulsion Laboratory, California Institute of Technology, under contract with the National Aeronautics and Space Administration.

References

- [1] E. T. Chatzichristou (2001) *Astrophys. J.* **556** 653.
- [2] J. Kormendy (1977) *Astrophys. J.* **217** 406.
- [3] N. V. Boris, C. J. Donzelli, M. G. Pastoriza, A. Rodriguez-Ardila, and D. L. Ferreiro (2002) *Astron. Astrophys.* **384** 780.
- [4] L. S. Slavcheva-Mihova, G. T. Petrov, and B. M. Mihov (2005) in Proceedings of the *Balkan Astronomical Meeting*, held June 14-18, 2004 in

Table 4: Ring parameters for Mrk 506.

| Code | μ_{cen} [mag / \square''] | r_{cen} [''] | \mathcal{FW} [''] |
|-------------------|---|----------------------------|--------------------------|
| 2bU | $24.119^{0.079}$ | $8.679^{0.118}$ | $4.874^{0.240}$ |
| 1bB | $24.140^{0.053}$ | $8.793^{0.086}$ | $3.430^{0.199}$ |
| 2bB | $23.750^{0.049}$ | $8.721^{0.098}$ | $4.035^{0.224}$ |
| 1bV | $22.754^{0.013}$ | $8.211^{0.027}$ | $4.926^{0.059}$ |
| 2bV | $22.999^{0.037}$ | $8.118^{0.073}$ | $4.656^{0.163}$ |
| 1b R_{C} | $22.451^{0.033}$ | $8.755^{0.086}$ | $4.356^{0.143}$ |
| 2b R_{C} | $22.167^{0.019}$ | $7.685^{0.041}$ | $5.392^{0.083}$ |
| 1b I_{C} | $21.469^{0.015}$ | $8.273^{0.043}$ | $4.959^{0.073}$ |
| 2b I_{C} | $21.640^{0.029}$ | $7.705^{0.057}$ | $5.443^{0.110}$ |

Rozhen NAO, Bulgaria; Space Research Institute: "Aerospace Research in Bulgaria" **20** 60.

- [5] J. L. Sérsic (1968) *Atlas de Galaxias Australes*, Observatorio Astronómico, Córdoba, Argentina.
- [6] K. C. Freeman (1970) *Astrophys. J.* **160** 811.
- [7] O. Bendinelli, G. Parmeggiani, and F. Zavatti (1982) *Astrophys. Sp. Sci.* **83** 239.
- [8] M. E. Bailey and W. B. Sparks (1983) *MNRAS* **204** 53P.
- [9] E. Laurikainen, H. Salo, and R. Buta (2005) *MNRAS* **362** 1319.
- [10] M. Prieto, J. A. L. Aguerri, A. M. Varela, and C. Muñoz-Tuñón (2001) *Astron. Astrophys.* **367** 405.
- [11] W. H. Press, B. P. Flannery, S. A. Teukolski, and W. T. Vetterling (1992) *Numerical recipes in C. The art of scientific computing*, Cambridge University Press, Cambridge.
- [12] H. Wozniak, D. Friedli, L. Martinet, P. Martin, and P. Bratschi (1995) *Astron. Astrphys. Suppl.* **111** 115.

- [13] M. Balcells, A. W. Graham, L. Domínguez-Palmero, and R. F. Peletier (2003) *Astrophys. J.* **582** L79.
- [14] J. A. L. Aguerri, N. Elias-Rosa, E. M. Corsini, C. Muñoz-Tuñón (2005) *Astron. Astrophys.* **434** 109.

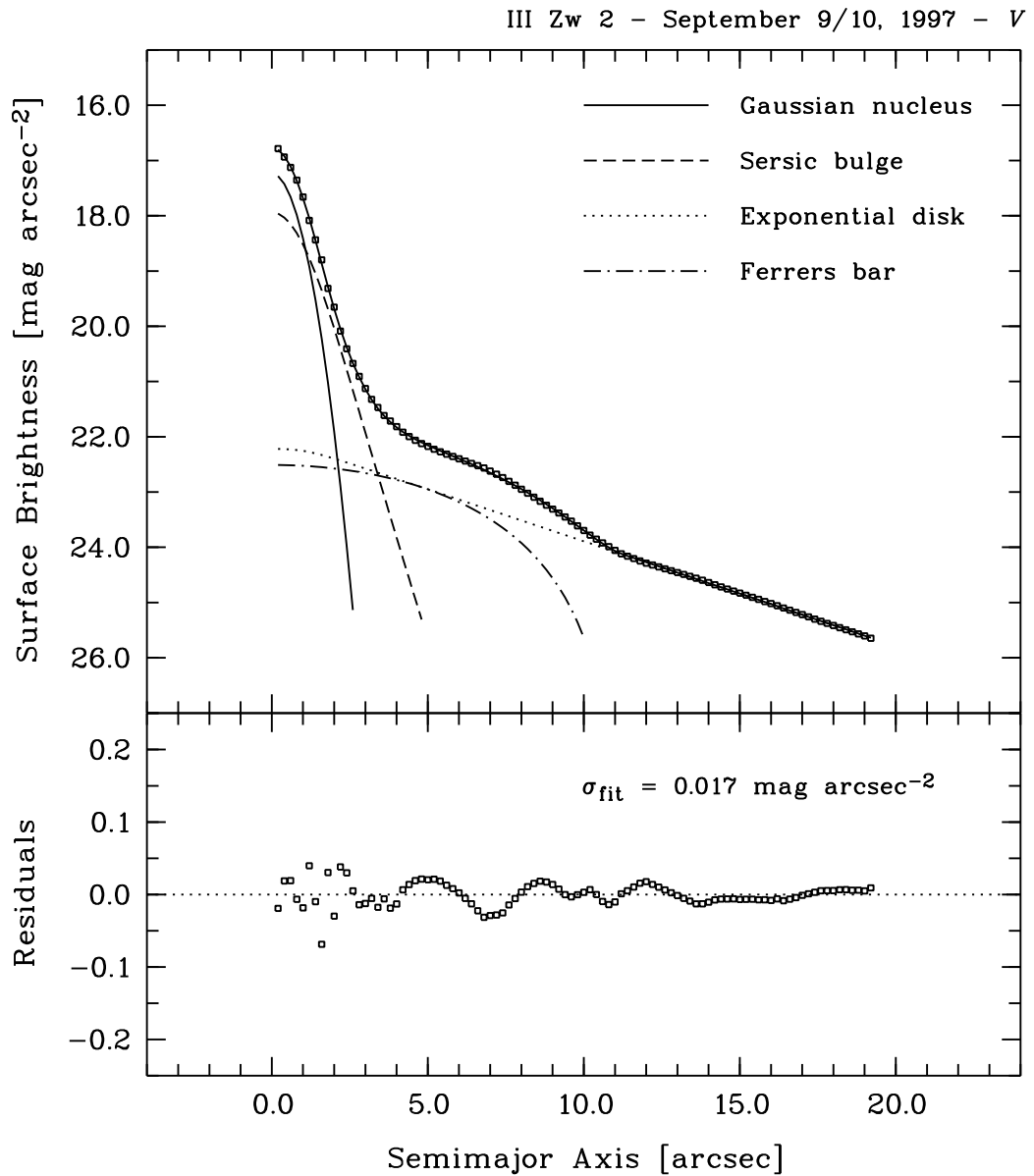


Figure 1: SBP decomposition for III Zw 2. In the upper panel the observed SBP (open squares) and the decomposed profiles of the structural components are shown; the resulting model SBP closely follows the observed one. In the lower panel the residual profile is shown.

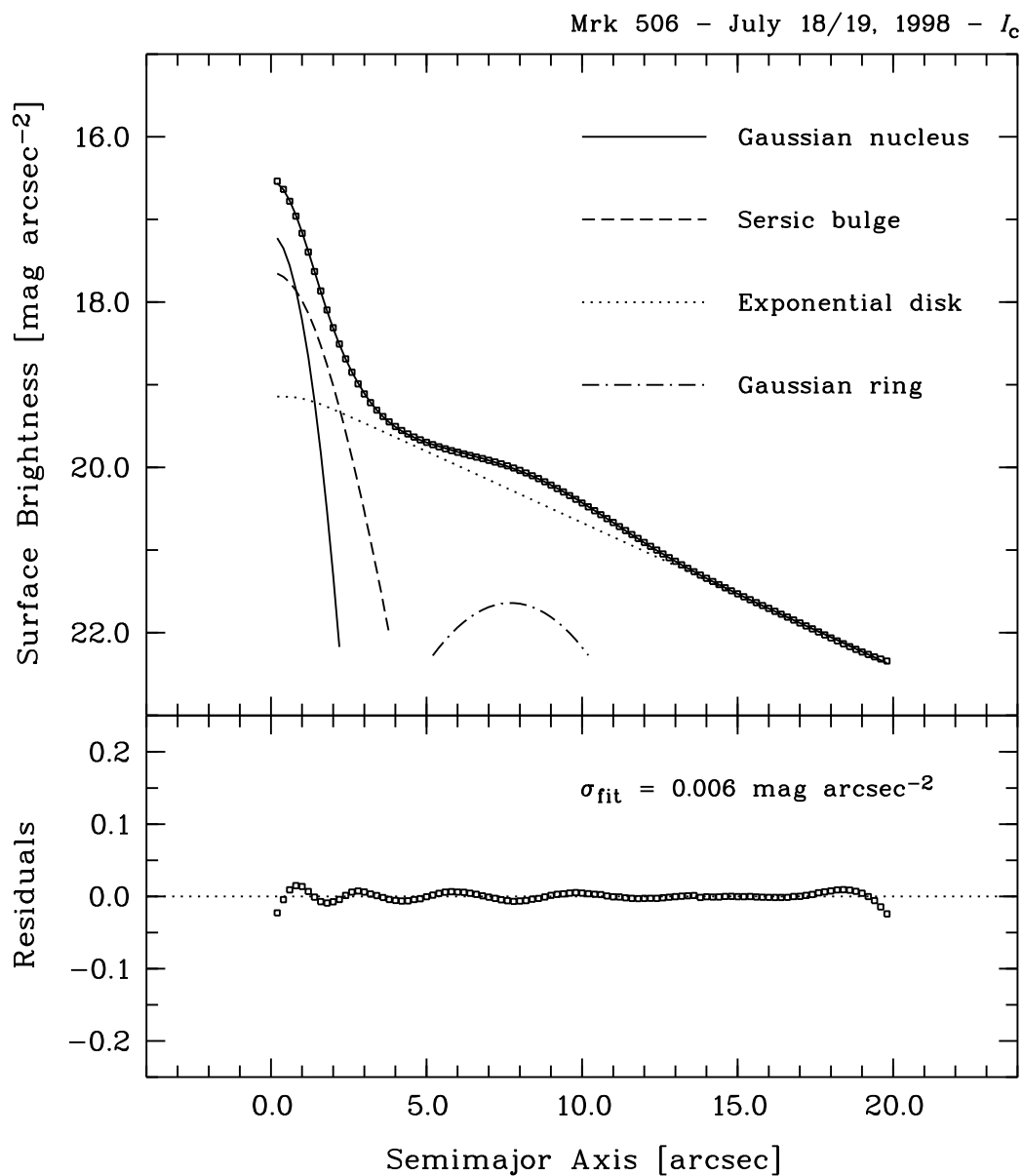


Figure 2: The same as in Fig 1 but for Mrk 506.

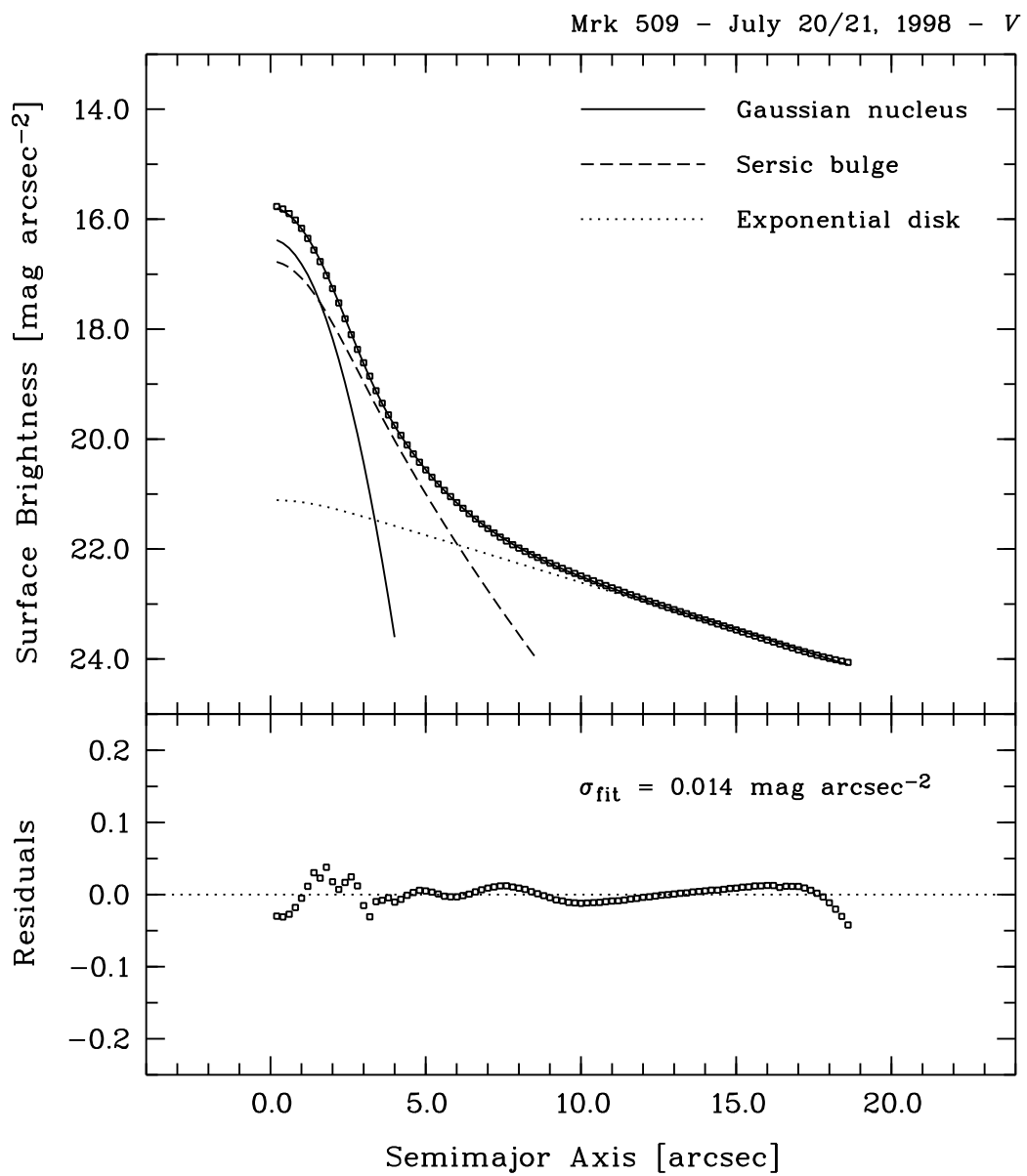


Figure 3: The same as in Fig 1 but for Mrk 509.